

# Modulation of Shock-End Virtual Electrode Polarisation as a Direct Result of 3D Fluorescent Photon Scattering

M.J. Bishop, B. Rodriguez, N. Trayanova & D.J. Gavaghan

**Abstract**—Due to the large transmural variation in transmembrane potential following the application of strong electric shocks, it is thought that fluorescent photon scattering from depth plays a significant role in optical signal modulation at shock-end. For the first time, a model of photon scattering is used to accurately synthesize fluorescent signals over the irregular geometry of the rabbit ventricles following the application of such strong shocks. A bidomain representation of electrical activity is combined with finite element solutions to the photon diffusion equation, simulating both the excitation and emission processes, over an anatomically-based model of rabbit ventricular geometry and fiber orientation. Photon scattering from within a 3D volume beneath the epicardial optical recording site is shown to transduce differences in transmembrane potential within this volume through the myocardial wall. This leads directly to a significantly modulated optical signal response with respect to that predicted by the bidomain simulations, distorting epicardial virtual electrode polarization produced at shock-end. Furthermore, we show that this degree of distortion is very sensitive to the optical properties of the tissue, an important variable to consider during experimental mapping set-ups. These findings provide an essential first-step in aiding the interpretation of experimental optical mapping recordings following strong defibrillation shocks.

## I. INTRODUCTION

Over the last decade, the optical mapping technique has revolutionized research in cardiac electrophysiology due to its unique ability to provide simultaneous, non-invasive recordings of transmembrane potential from multiple sites over the surface of the heart. The technique uses voltage-sensitive fluorescent dyes that bind to the membranes of excitable cardiac cells [1]. Upon illumination at the correct wavelength, these dye molecules become excited and fluoresce, transducing changes in the transmembrane potential as changes in fluorescent emission. However, as the illuminating light penetrates deeply into the myocardium (up to a few millimeters [2]), the detected signal contains fluorescent photons originating not only from several millimetres directly beneath the recording site [2], but also from a widely distributed 3D volume surrounding it (which we will term the *scattering volume*), with the photons encountering multiple scattering events in the tissue prior to exiting the surface [3].

This work was supported by the United Kingdom Engineering and Physical Sciences Research Council (EPSRC) through a Life Sciences Interface Doctoral Training Centre studentship for MJB (GR/S58119/01) and the Integrative Biology e-science pilot project (DJG, GR/S72023/01), in addition to the National Institutes of Health grants HL063195, HL074283, and HL067322 (NT).

M.J. Bishop, B. Rodriguez and D.J. Gavaghan are with the Computational Biology Group, University of Oxford, Oxford, UK david.gavaghan@comlab.ox.ac.uk

N. Trayanova is with the Department of Bioengineering, Tulane University, New Orleans, LA, USA

Previous modelling studies have successfully shown that distortional effects seen in experimentally recorded optical action potential upstrokes and activation wavefront widths can be directly attributed to fluorescent photon scattering from within the scattering volume beneath the epicardial recording site [4], [5], [6], [7]. Differences in potential within this volume as the wavefront passes through are transduced through the myocardial wall by photon scattering, distorting the optical signal recorded from the surface. Furthermore, the size of the scattering volume has been shown to be a sensitive function of the optical properties of the tissue at both the illumination and emission wavelengths, thus affecting the degree of distortion seen in the recorded signal [7].

Optical mapping is the only experimental technique capable of accurately studying the response of cardiac tissue to strong electric shocks, allowing recordings to be made during the shock and immediately after shock application, due to the absence of stimulus-induced artifacts present in micro-electrode recordings. It has been hypothesised that modulation of fluorescent recordings by photon scattering will be particularly important following the application of such strong defibrillation shocks [7] where there is a highly irregular transmembrane potential distribution through the myocardial wall, beneath the optical recording site [8], [9]. It is the goal of this study to directly investigate the effect of fluorescent photon scattering from depth upon the synthesized optical signals obtained following such protocols, and specifically the way in which such heterogeneous transmembrane potential distributions through the mid-myocardium effect optically recorded shock-end virtual electrode polarization (VEP). Furthermore, the dependence of the optical signal modulation upon the scattering properties of the tissue in such instances is assessed. To do so, we use a novel anatomically-based finite element rabbit ventricular model, which combines a bidomain model of electrical activity with a photon transport model of illumination and fluorescence, presented in our previous study [7].

## II. METHODS

The anatomically-based finite element model of the rabbit ventricles described in a previous study [10] was used to solve the equations governing both electrical activation and photon scattering during the processes of illumination and emission. The myocardial mesh incorporated realistic geometry and fiber orientation, and also included representation of the perfusing bath and the blood in the ventricular cavities.

The distribution of transmembrane potential ( $V_m$ ) throughout the ventricles was calculated using the bidomain equa-

tions, the details of which have been described extensively elsewhere [10]. Membrane kinetics were represented by the augmented Luo-Rudy dynamic model for defibrillation [11]. A stimulus of twice threshold and 4ms duration was applied at an epicardial site with a 2cm<sup>2</sup> electrode located at the apex at a basic cycle length of 250ms. At various coupling intervals (CI) following the 8th pacing stimulus, monophasic shocks of various shock strengths (SS) and of 8ms duration were applied via two large mesh electrodes located at the vertical boundaries of the perfusing bath, as described in [9].

We calculated both the photon density due to uniform excitation illumination and the photon density due to voltage-sensitive fluorescent emission at all points within the 3D volume of the ventricles using the steady-state photon diffusion equation, using the method described in our previous study [7]. The optical properties of the tissue at both illumination and emission wavelengths were represented by penetration depths of 0.90mm and 2.10mm, respectively. Both the transmembrane potential  $V_m$ , and the synthesized optical signal  $V_{opt}$ , were normalized at each epicardial surface node in the finite element mesh using the maximum and minimum action potential values for that node following pacing, as in experimental recordings [12]. We defined the upstroke duration of the action potential as the time interval between 10 and 90 percent of depolarization.

### III. RESULTS

Fig. 1 shows the timecourse of the transmembrane potential  $V_m$  (blue) and the synthesized optical signal  $V_{opt}$  (red) recorded from a node on the anterior epicardial surface of the right ventricle (RV) during the stimulation protocol described in the Methods. In the case shown, SS = 17V/cm and CI = 140ms. Following the pacing stimulus (first 140ms of Fig. 1), the main difference between the  $V_m$  and  $V_{opt}$  traces occurs during the action potential upstroke, with the optical upstroke (duration 6.9ms) being prolonged with respect to the transmembrane upstroke (1.5ms). During the shock the response of  $V_{opt}$  is significantly reduced with respect to that of  $V_m$ . The resulting level of maximum polarization following the shock, measured at shock-end and normalized with respect to the pacing action potential amplitude, is 0.93 for  $V_{opt}$  compared to 1.83 for  $V_m$ , for the particular node shown.

Fig. 2 depicts shock-end distributions of  $V_m$  (left) and  $V_{opt}$  (right) across the anterior epicardial surface of the ventricles for four shocks (CI and SS is specified on the left of each panel). In addition to the epicardial polarization, the  $V_m$  panel also shows transmural views of  $V_m$  distribution. Histograms show the percentage of nodes within the window on the anterior surface of the ventricles (depicted in the 11V/cm 120ms  $V_m$  image, and which represents the approximate field of view from the detector array in experiments [9]) which are either: a) depolarized ( $> 1$ ), b) of intermediate polarization ( $0 - 1$ ), or c) hyperpolarized ( $< 0$ ).

In both  $V_m$  and  $V_{opt}$  images of Fig. 2, the effect of the shock is to induce two main areas of opposite in-sign

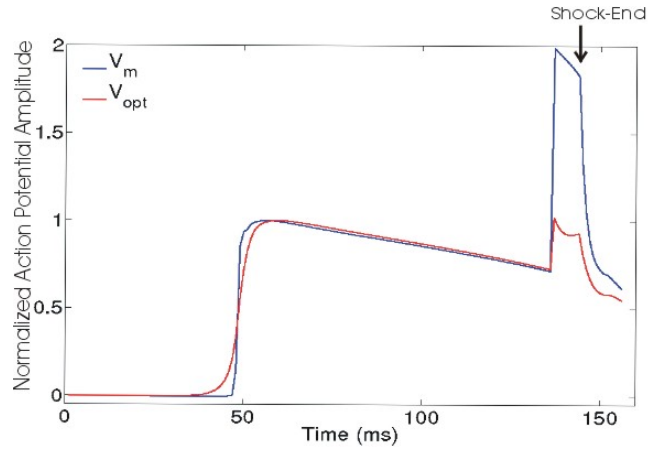


Fig. 1. Timecourse of  $V_m$  (blue) and  $V_{opt}$  (red) for a selected node on the anterior epicardial surface of the RV during a stimulation protocol with SS = 17 V/cm and CI = 140ms.

virtual-electrode polarization (VEP) across the epicardium, as demonstrated in previous studies [9], [13]. The left ventricle (LV) surface which is near the cathode is hyperpolarized (polarization levels  $< 0$  - blue in the colour scheme), and the RV surface which is near the anode is depolarized (polarization levels  $> 1$  - red in the colour scheme), with a region of surface nodes of intermediate polarization in between. Inclusion of the averaging effects of photon scattering in  $V_{opt}$  results in apparently weaker VEP with a larger percentage of nodes with intermediate polarization compared to  $V_m$ , which is quantified by the histograms of Fig. 2.

Consistent with previous studies [8], [9], examination of the transmural  $V_m$  images of Fig. 2 show that the shock induces a complex distribution of  $V_m$  in the depth of the ventricular wall, with the endocardial surface in both the LV and RV having opposite polarization to the corresponding epicardial polarization. Between the oppositely polarized endocardium and epicardium, the intramural wall is of intermediate polarization levels (largely green and yellow in the colour scheme) in both the RV and LV, occurring for all SS/ CI protocols.

Fig. 3 shows the maximum and minimum values of normalized polarization found within the anterior epicardial surface window (shown in Fig. 2) at shock-end for both  $V_m$  and  $V_{opt}$ . Again, we see a large modulation in the maximum response of the  $V_{opt}$  signal to the shock, compared to the  $V_m$  response. Furthermore, the range of normalized  $V_m$  polarization values is seen to increase with SS, being 1.88 and 1.90 for a SS of 11V/cm and 2.70 and 2.72 for 17V/cm, for CI of 120 and 140ms, respectively. In the optical response, we see a similar relative change with SS, being 0.85 and 0.97 for a SS of 11V/cm and 1.20 and 1.33 for 17V/cm, for CI of 120 and 140ms, respectively.

It has been shown in a previous study that the distortion caused by fluorescent photon scattering depends sensitively upon the values of the optical properties of the tissue during both illumination and emission [7]. Fig. 4 plots the variation in the maximum range of polarization values in the optical

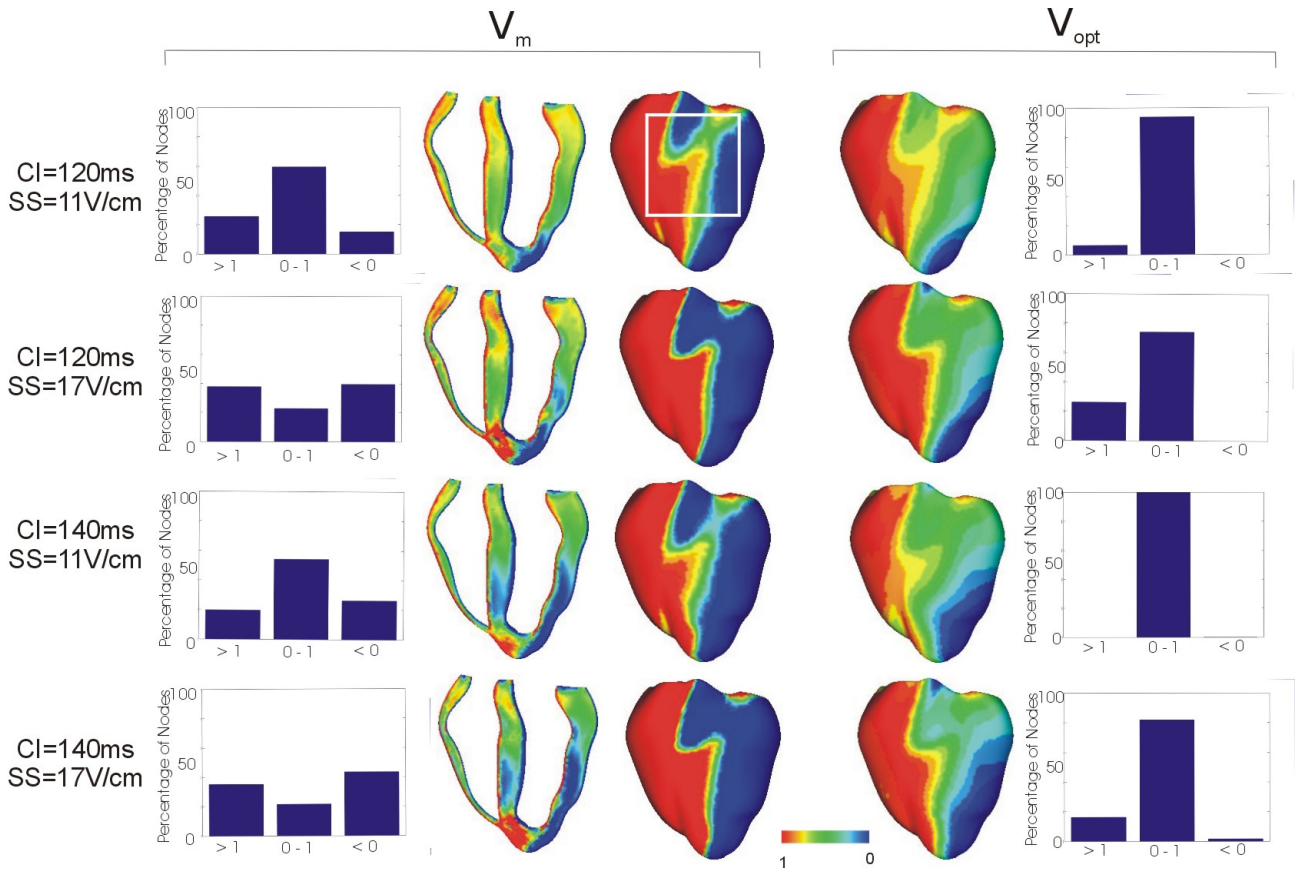


Fig. 2. Shock-end VEP images showing epicardial polarization distributions for  $V_m$  (left) and  $V_{opt}$  (right) as well as transmural potential distributions (for  $V_m$ ). Histograms show percentage of nodes with polarizations  $> 1$ ,  $0 - 1$  and  $< 0$  within the anterior epicardial window shown in the upper  $V_m$  image.

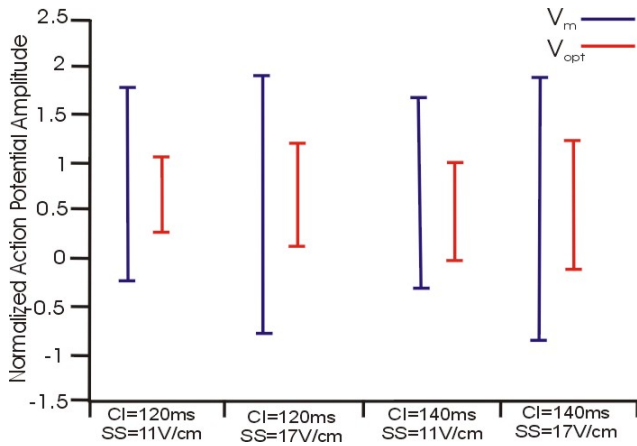


Fig. 3. Maximum and minimum shock-end values of normalized polarization levels found within the the anterior epicardial window shown in Fig. 2.

signal found within the anterior window shown in Fig. 2 (maximum minus minimum value), as the scattering properties of the tissue are varied. This is achieved by altering the penetration depths during illumination and emission by a certain fraction, relative to the default values of 0.90mm and 2.10mm, respectively. As penetration depths vary by relative fractions of between 0.5 and 1.5, the amplitude of the

maximum-minimum response in  $V_{opt}$  is seen to vary between 1.79 and 1.06.

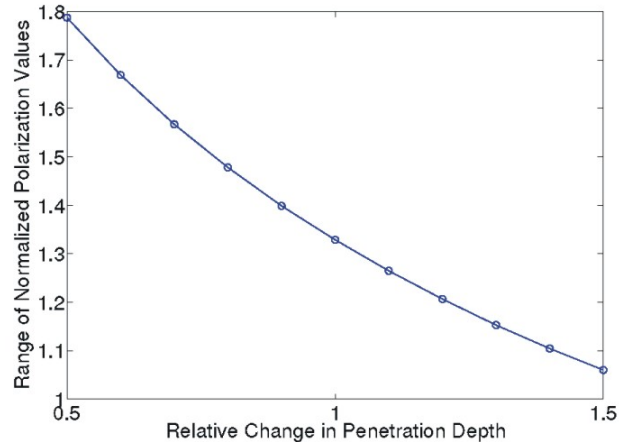


Fig. 4. Variation in the range of normalized  $V_{opt}$  values ( $V_{opt}^{max} - V_{opt}^{min}$ ) found within the anterior window in the optical shock-end images of Fig. 2 as the scattering properties of the tissue are varied.

#### IV. DISCUSSION

In this study, a model of photon scattering for illumination and emission is used in combination with an anatomically-

based bidomain model of the rabbit ventricles to simulate fluorescent signals over the entire epicardium. We use this model to investigate the role of photon scattering in modulating optical signals following the application of strong electric shocks.

Fluorescent photon scattering results in distortion of the optically recorded signal. This distortion is particularly apparent when there is a largely heterogeneous transmural distribution of transmembrane potential within the scattering volume beneath the surface recording site. Variations in the level of polarization within the scattering volume are transduced through the mid-myocardium by the scattered photons. This characteristic averaging effect results in differences in the epicardial  $V_{opt}$  polarizations to those predicted by bidomain simulations of  $V_m$ . Our results have shown that this effect is particularly apparent in the case of shock-end VEP measurements, where there is a complete switch of polarization between epi- and endocardium through the myocardial wall, with the mid-myocardium being of intermediate polarization. We have demonstrated that the specific distribution of polarization values in the mid-myocardium, close to the epicardial surface, is thus critically important in determining the degree of modulation of the optical signal.

The resulting large transition region between areas of opposite polarization on the LV and the RV across the anterior epicardial surface in the shock-end VEPs images of  $V_{opt}$  compared to  $V_m$ , agrees qualitatively with those witnessed in experimentally recorded optical VEP images [14], [9]. We strongly believe the results presented in this study provide the opportunity to explain previously seen differences between experimental VEPs and those from bidomain simulations [9] by directly accounting for photon scattering from depth.

In a previous study we have demonstrated the way in which variations in the optical properties of the myocardium at both the illumination and emission wavelengths effect the distortion of the optical action potential upstroke duration. Here we have shown that this effect is even more significant when applied to analysis of potential distributions occurring following a strong shock. As the penetration depths at both the emission and illumination wavelengths are varied, we are effectively changing the dimensions of the 3D scattering volume from which scattered photons, recorded in the optical signal, originate from. These scattered photons convey information about the different levels of polarization within the scattering volume, becoming apparent as a distortion of the surface optical signal. Following a strong shock, there are large variations in potential through the myocardium. Therefore, even small changes in this 3D volume, as penetration depths change by just  $\pm 50\%$  (commonly encountered in different tissue types), result in the large changes seen in the modulation effects in the optical signal due to fluorescent photon scattering.

## V. CONCLUSION

In conclusion, this study provides insight into the mechanisms and underlying physical processes responsible for the blurring and distortion effects seen in experimentally

recorded optical signals as a direct result of fluorescent photon scattering following the application of strong shocks. The use of accurate ventricular geometry and fiber orientation in the model is essential in representing the complex pattern of potential distribution following such shock protocols. In this study we have presented, for the first time, an essential first-step in aiding in the interpretation of the experimental optical mapping recordings following strong defibrillation shocks.

## REFERENCES

- [1] L.M. Loew, "Optical mapping of cardiac excitation and arrhythmias", in *Mechanisms and principles of voltage sensitive fluorescence*, eds. D.S. Rosenbaum and J. Jalife, Futura Publishing, Armonk, NY, 2001, pp. 33-46
- [2] W.T. Baxter, S.F. Mironov, A.V. Zaitsev, J. Jalife and A.M. Pertsov, Visualizing excitation waves in cardiac muscle during ransillumination, *Biophys. J.*, vol. 80, 2001, pp. 516-530
- [3] L. Ding, R. Splinter and S. Knisley, Quantifying spatial localization of optical mapping using Monte Carlo simulations, *IEEE Trans. Biomed. Eng.*, vol. 48 (10), 2001, pp. 1098-1107
- [4] C.J. Hyatt, S.F. Mironov, M. Wellner, O. Berenfeld, A.K. Popp, D.A. Weitz, J. Jalife and A.M. Pertsov, Synthesis of voltage-sensitive fluorescence signals from three-dimensional myocardial activation patterns, *Biophys. J.*, vol. 85, 2003, pp. 2673-2683
- [5] M.A. Bray, and J.P. Wikswo, Examination of optical depth effects on fluorescence imaging of cardiac propagation, *Biophys. J.*, vol. 85, 2003, pp. 4134-4145
- [6] C.J. Hyatt, S.F. Mironov, F.J. Vetter, C.W. Zemlin and A.M. Pertsov, Optical action potential upstroke morphology reveals near-surface transmural propagation direction, *Circ. Res.*, vol. 97, 2005, pp. 277-284
- [7] M.J. Bishop, B. Rodriguez, J. Eason, J.P. Whiteley, N. Trayanova and D.J. Gavaghan, Synthesis of voltage-sensitive optical signals: Application to panoramic optical mapping, *Biophys. J.*, vol. 90, 2006, pp. 2938-2945
- [8] B. Rodriguez and N. Trayanova, Upper limit of vulnerability in a defibrillation model of the rabbit ventricles, *J. Electrocardiol.*, vol. 36, 2003, pp. 51-56
- [9] B. Rodriguez, L. Li, J.C. Eason, I.R. Efimov and N. Trayanova, Differences between left and right ventricular chamber geometry affect cardiac vulnerability of electric shocks, *Circ. Res.*, vol. 97, 2005, pp. 168-175
- [10] N. Trayanova, J. Eason and F. Aguel, Computer simulations of cardiac defibrillation: a look inside the heart, *Comput. Visual. Sci.*, vol. 4, 2002, pp. 259-270
- [11] T. Ashihara and N.A. Trayanova, Asymmetry in membrane responses to electric shocks: insights from bidomain simulations, *Biophys. J.*, vol. 87(4), 2004, pp. 2271-82
- [12] I.R. Efimov, V. Sidorov, Y. Cheng and B. Wollenzier, Evidence of three-dimensional scroll waves with ribbon-shaped filaments as a mechanism of ventricular tachycardia in isolated rabbit heart, *J. Cardiovasc. Electrophysiol.*, vol. 10, 1999, pp. 1451-1462
- [13] I.R. Efimov, F. Aguel, Y. Cheng, B. Wollenzier and N. Trayanova, Virtual electrode polarization in the far field: implications for external defibrillation, *Am. J. Physiol. Heart. Circ. Physiol.*, 279, 2000, H1055-H1070
- [14] I.R. Efimov, R.A. Gray and B.J. Roth, Virtual electrodes and de-excitation: new insights into fibrillation induction and defibrillation, *J. Cardiovasc. Electrophysiol.*, vol. 11, 2000, pp. 339-353